SIAM J. SCI. COMPUT.
Vol. 38, No. 4, pp. A1919–A1934

AN INVARIANT PRESERVING DISCONTINUOUS GALERKIN METHOD FOR THE CAMASSA–HOLM EQUATION*

HAILIANG LIU† AND YULONG XING‡

Abstract. In this work, we design, analyze, and numerically test an invariant preserving discontinuous Galerkin method for solving the nonlinear Camassa–Holm equation. This model is integrable and admits peakon solitons. The proposed numerical method is high order accurate, and preserves two invariants, momentum and energy, of this nonlinear equation. The L^2-stability of the scheme for general solutions is a consequence of the energy preserving property. The numerical simulation results for different types of solutions of the Camassa–Holm equation are provided to illustrate the accuracy and capability of the proposed method.

Key words. discontinuous Galerkin method, Camassa–Holm equation, energy conservation, stability

AMS subject classifications. 65M60, 65M12, 35Q53

DOI. 10.1137/15M102705X

1. Introduction.

In this paper, we are interested in accurate numerical approximations to the nonlinear Camassa–Holm (CH) equation:

$$m_t + um_x + 2mu_x = 0, \quad m = u - u_{xx}, \quad x \in \mathbb{R},\ t > 0, \tag{1}$$

where the subscript t (or x, respectively) denotes the differentiation with respect to time variable t (or x). By taking advantage of its Hamiltonian structure to reformulate this equation, we develop an invariant preserving discontinuous Galerkin method for this nonlinear CH equation. Our proposed scheme is high order accurate, and preserves two invariants, momentum and energy, of this nonlinear equation, hence producing wave solutions with satisfying long time behavior.

The CH equation was found in a study by Camassa and Holm [4], as a bi-Hamiltonian model for waves in the shallow water. In this context, the equation takes the form

$$u_t + 2ku_x - u_{xxt} + 3uu_x = 2u_xu_{xx} + uu_{xxx}. \tag{2}$$

If the parameter k is positive, the solitary wave solutions are smooth solitons. In the special case that $k = 0$, equation (2) reduces to the CH equation (1), which has peakon solutions: solitons with a sharp peak, containing a discontinuity at the peak in the wave slope profile. Equation (2) can also be written as the system of equations

$$\begin{aligned} &u_t + uu_x + p_x = 0, \\ &p = (1 - \partial_x^2)^{-1}\left(2ku + u^2 + \frac{1}{2}(u_x)^2\right), \end{aligned}$$

*Submitted to the journal's Methods and Algorithms for Scientific Computing section June 22, 2015; accepted for publication (in revised form) March 22, 2016; published electronically July 6, 2016.

http://www.siam.org/journals/sisc/38-4/M102705.html

†Department of Mathematics, Iowa State University, Ames, IA 50011 (hliu@iastate.edu). This author's work was supported by the National Science Foundation under grant DMS-1312636 and by NSF grant RNMS (Ki-Net) 1107291.

‡Department of Mathematics, University of California at Riverside, Riverside, CA 92521 (xingy@ucr.edu). This author's work was supported by NSF grant DMS-1216454.

with p being the dimensionless pressure or surface tension.

This nonlocal CH equation is also one of three equations in the family

$$u_t - \alpha^2 u_{xxt} + \gamma u_{xxx} + c_0 u_x = (c_1 u^2 + c^2 u_x^2 + c_3 u u_{xx})_x,$$

which satisfies "asymptotic integrability up to third order," a necessary condition for the complete integrability. The other two cases in this family are the Korteweg–de Vries (KdV) equation,

$$u_t + u u_x + u_{xxx} = 0,$$

and the Degasperis–Procesi (DP) shallow water equation,

$$u_t - u_{xxt} + 3 u u_x = u u_{xxx} + 2 u_x u_{xx}.$$

The CH equation and DP equation also belong to the θ-class of dispersive models:

$$u_t - u_{txx} + u u_x = \theta u u_{xxx} + (1-\theta) u_x u_{xx},$$

with $\theta = 1/3$ and $1/4$, respectively. The θ-class was first identified in [20], as a subclass of those introduced in [19] and the analysis on its global existence versus finite wave breaking was given by Liu and Yin [23] with the following results: for $\frac{1}{2} \le \theta \le 1$, initial smoothness is shown to persist for all time; if $0 \le \theta < \frac{1}{2}$, strong solutions of the θ-equation may lose certain regularity in finite time, and traveling waves such as periodic, solitary, peakon, peaked periodic, cusped periodic, or cusped soliton are all permissible [18, 15].

The two special equations, the CH and DP equations, in the θ-class share several interesting properties including the bi-Hamiltonian structure, the complete integrability, and the soliton-like peakon solutions. Both equations can be viewed as models of shallow water waves [13, 4, 5, 17, 11, 16, 10]. However, there are also important differences between these equations: from the perspective of PDE theory, the solutions of the CH equation basically belong to $H^1(\mathbb{R})$ (the first order Sobolev space), while the DP equation can develop shocks (jump discontinuities) which may be understood as entropy solutions [8, 9, 24].

For the CH equation with any initial data $u_0 \in H^1(\mathbb{R})$, various papers have studied the global existence of its solutions, conservative or dissipative. Uniqueness is a delicate issue because in general the flow map has less regularity than usually needed to justify the uniqueness of the solution. Recently, Bressan, Chen, and Zhang [2] proved that the Cauchy problem of the CH equation with general initial data $u_0 \in H^1(\mathbb{R})$ has a unique, globally in time, conservative solution. The energy conservation property is essentially used in their uniqueness proof to overcome certain difficulty.

We plan to compute this unique conservative solution numerically by the discontinuous Galerkin (DG) method. The DG method is a class of finite element methods using discontinuous piecewise polynomial spaces for both the numerical solutions and the test functions (see [7] for a historic review). It combines advantages of both finite volume and finite element methods, and has been successfully applied to a wide range of applications. Many DG methods have been designed for various water wave equations. Some examples can be found in the review paper [28]. An energy dissipative DG method for the CH equation has been presented in [27]. Recently, there have been some studies on invariant preserving DG methods, which can preserve the mass and energy exactly in the discrete sense. Numerical evidence shows that such methods often provide more accurate results in long time simulations. Invariant preserving DG methods have been designed for various wave equations including the KdV equation

[3, 29], second order wave equation [26, 6], and the DP equation [21]. We also refer the interested reader to [25, 14, 1] for some related methods for second order acoustic wave equations.

The goal of this paper is to develop a novel DG method for the CH equation, to preserve both the momentum and energy, which are given by

$$E_1 = \int_{\mathbb{R}} (u - u_{xx}) dx, \quad E_2 = \frac{1}{2} \int_{\mathbb{R}} \left(u^2 + u_x^2\right) dx$$

or

$$E_1 = \int_{\mathbb{R}} m dx, \quad E_2 = \frac{1}{2} \int_{\mathbb{R}} mu dx.$$

with $m = u - u_{xx}$. The local DG method introduced in [27] uses the following reformulation:

$$\begin{aligned} m_t + f(u)_x - p_x + (r^2/2)_x &= 0, \\ p - (ru)_x &= 0, \end{aligned}$$

where $f(u) = 3u^2/2$ and $r = u_x$. The Lax–Friedrichs flux for $f(u)$ used in [27] is held accountable for the dissipation of the energy E_2. In this work we explore yet another reformulation

$$\begin{aligned} m_t + q_x + mr &= 0, \\ q - mu &= 0, \end{aligned}$$

which takes advantage of the first compatible Hamiltonian description

$$m_t = -D_1 \frac{\partial E_2}{\partial m} \quad \text{for} \quad D_1 = \partial_x m + m \partial_x. \tag{3}$$

This, together with simple central numerical fluxes, makes it possible that the resulting scheme preserves both the momentum and energy. Besides the high order of accuracy, one main feature of the scheme is its capability to produce wave solutions with satisfying long time behavior. Some comparison shows that the scheme which conserves these two quantities has smaller phase error than those produced by the energy dissipative scheme. With P^0 elements, the DG discretization in the present work may be viewed as a finite difference scheme such as the one studied in [22], thus extending the results for the scalar CH equation obtained in [22]. Finally, we point out that the CH equation also admits another compatible Hamiltonian description

$$m_t = -\partial_x \frac{\partial E_3}{\partial u} \quad \text{for} \quad E_3 = \frac{1}{2} \int_{\mathbb{R}} u \left(u^2 + u_x^2\right) dx.$$

This work shows that the scheme conserving both E_1 and E_2 is clearly better than that which conserves only E_1. One would intuitively think it is even better to preserve E_1, E_2, and E_3. However, it appears a rather difficult task to preserve all three conservation laws, yet still maintain the optimal order of convergence for smooth solutions.

The rest of this paper is organized as follows. In section 2, we formulate our DG method in both semidiscrete and fully discrete setting, and prove the desired invariant preserving properties of the proposed DG method. In section 3, we present a set of numerical examples to illustrate the capacity of the DG scheme to capture various peakons and their interactions. Some conclusion remarks are given in section 4.

2. The discontinuous Galerkin methods.

2.1. Reformulation. The Hamiltonian description (3) sets the basis to construct an E_2 preserving discretization for (1), and it leads to the following reformulation:

$$m_t + (mu)_x + mu_x = 0, \quad m = u - u_{xx}. \tag{4}$$

By introducing the auxiliary variables r and q, we rewrite this form into the following system:

$$m_t + q_x + mr = 0, \tag{5a}$$
$$q - mu = 0, \tag{5b}$$
$$m - u + r_x = 0, \tag{5c}$$
$$r - u_x = 0. \tag{5d}$$

Two conservation laws for the CH equation can be expressed as

$$E_1 = \int_{\mathbb{R}} m dx, \quad E_2 = \frac{1}{2}\int_{\mathbb{R}} mu dx = \frac{1}{2}\int_{\mathbb{R}} (u^2 + r^2) dx. \tag{6}$$

2.2. DG formulation. We develop an invariant preserving DG method for the CH equation subject to initial data $u_0(x)$ and periodic boundary conditions. Let us denote the computational mesh of the domain I by $I_j = (x_{j-1/2}, x_{j+1/2})$ for $j = 1, \ldots, N$. The center of the cell is $x_j = (x_{j-1/2} + x_{j+1/2})/2$, and $h_j = x_{j+1/2} - x_{j-1/2}$. We denote by $w^+_{j+1/2}$ the value of w at $x_{j+1/2}$ evaluated from the right element I_{j+1}, and $w^-_{j+1/2}$ the value of w at $x_{j+1/2}$ evaluated from the left element I_j. $[w] = w^+ - w^-$ denotes the jump of w at cell interfaces, and $\{w\} = \frac{1}{2}(w^+ + w^-)$ denotes the average of the left and right interface values. We then define the piecewise polynomial space V_h as the space of polynomials of degree k in each cell I_j, i.e.,

$$V_h = \{w : w \in P^k(I_j) \text{ for } x \in I_j, j = 1, \ldots, N\}.$$

The DG method for (5) is formulated as follows: for all the test functions $\xi_h, \eta_h, \rho_h, \psi_h \in V_h$, find $m_h, q_h, r_h, u_h \in V_h$ such that

$$\int_{I_j} (m_h)_t \xi_h dx - \int_{I_j} q_h (\xi_h)_x dx + \left(\hat{q}_h \xi_h^-\right)_{j+1/2} - \left(\hat{q}_h \xi_h^+\right)_{j-1/2} + \int m_h r_h \xi_h dx = 0, \tag{7a}$$

$$\int_{I_j} (q_h - m_h u_h)\eta_h dx = 0, \tag{7b}$$

$$\int_{I_j} m_h \rho_h dx - \int_{I_j} r_h (\rho_h)_x dx + \left(\hat{r}_h \rho_h^-\right)_{j+1/2} - \left(\hat{r}_h \rho_h^+\right)_{j-1/2} - \int_{I_j} u_h \rho_h dx = 0, \tag{7c}$$

$$\int_{I_j} r_h \psi_h dx + \int u_h (\psi_h)_x dx - \left(\hat{u}_h \psi_h^-\right)_{j+1/2} + \left(\hat{u}_h \psi_h^+\right)_{j-1/2} = 0. \tag{7d}$$

The "hat" terms, known as numerical fluxes, take only single values on cell interfaces given by

$$(\hat{q}_h, \hat{r}_h, \hat{u}_h) = (\{q_h\}, \{r_h\}, \{u_h\})\,. \tag{8}$$

The global form of the DG formulation may be obtained by summing over all the cells I_j,

$$\int (m_h)_t \xi_h dx - \int q_h (\xi_h)_x dx - \sum_{j=1}^{N} \left(\hat{q}_h [\xi_h]\right)_{j+1/2} + \int m_h r_h \xi_h dx = 0, \tag{9a}$$

$$\int (q_h - m_h u_h)\eta_h dx = 0, \tag{9b}$$

$$\int m_h \rho_h dx - \int r_h (\rho_h)_x dx - \sum_{j=1}^{N} \left(\hat{r}_h [\rho_h]\right)_{j+1/2} - \int u_h \rho_h dx = 0, \tag{9c}$$

$$\int r_h \psi_h dx + \int u_h (\psi_h)_x dx + \sum_{j=1}^{N} \left(\hat{u}_h [\psi_h]\right)_{j+1/2} = 0, \tag{9d}$$

where $\int = \sum_{j=1}^{N} \int_{I_j}$, and the periodic boundary conditions have been used.

2.3. Stability and conservative properties. We now turn to establish the conservation of E_1 and E_2.

Theorem 2.1. Let (m_h, q_h, u_h, r_h) be the numerical solutions of the DG formulation (7)–(8). Then we have the following:
(i) Both invariants E_1 and E_2 are preserved in the sense that

$$\frac{d}{dt}\int m_h dx = 0, \quad \frac{d}{dt}\int (u_h^2 + r_h^2) dx = 0.$$

(ii) The DG scheme is L^2 stable:

$$\|u_h(t)\|^2 \le \|u_0\|_{H^1}^2 \quad \forall\, t > 0.$$

Proof. (i) To show that the scheme preserves E_1, we simply take $\xi_h = 1$ in (9a), $\rho_h = -r_h$ in (9c), and $\psi_h = -u_h$ in (9d), and sum the resulting relations to obtain

$$\begin{aligned}
\frac{d}{dt}\int m_h dx &= -\int r_h (r_h)_x dx - \sum_{j=1}^{N} \left(\hat{r}_h [r_h]\right)_{j+1/2} + \int u_h (u_h)_x dx + \sum_{j=1}^{N} \left(\hat{u}_h [u_h]\right)_{j+1/2} \\
&= \sum_{j=1}^{N} \left(\left[\frac{r_h^2}{2}\right] - \hat{r}_h [r_h] - \left[\frac{u_h^2}{2}\right] + \hat{u}_h [u_h] \right)_{j+1/2} \\
&= \sum_{j=1}^{N} \left((\{r_h\} - \hat{r}_h)[r_h] - (\{u_h\} - \hat{u}_h)[u_h] \right)_{j+1/2} = 0.
\end{aligned}$$

To show the conservation of E_2, we take $\xi_h = u_h$ in (9a), $\eta_h = r_h$ in (9b), $\rho_h = -u_h$

in the time derivative of (9c), $\psi_h = (r_h)_t$ in (9d), and $\psi_h = -q_h$ in (9d) to obtain

$$\int (m_h)_t u_h dx - \int q_h (u_h)_x dx - \sum_{j=1}^{N} \left(\hat{q}_h [u_h]\right)_{j+1/2} + \int m_h r_h u_h dx = 0,$$

$$\int q_h r_h dx - \int m_h r_h u_h dx = 0,$$

$$- \int (m_h)_t u_h dx + \int (r_h)_t (u_h)_x dx + \sum_{j=1}^{N} \left((\hat{r}_h)_t [u_h]\right)_{j+1/2} + \int (u_h)_t u_h dx = 0,$$

$$\int r_h (r_h)_t dx + \int u_h (r_h)_{tx} dx + \sum_{j=1}^{N} \left(\hat{u}_h [(r_h)_t]\right)_{j+1/2} = 0,$$

$$- \int r_h q_h dx - \int u_h (q_h)_x dx - \sum_{j=1}^{N} \left(\hat{u}_h [q_h]\right)_{j+1/2} = 0.$$

Adding the above together and integrating the complete derivative out, we get

$$\frac{1}{2}\frac{d}{dt}\int \left(u_h^2 + r_h^2\right) dx = \sum_{j=1}^{N} \left(\hat{q}_h [u_h] + \hat{u}_h [q_h] - [u_h q_h]\right)_{j+1/2} + \sum_{j=1}^{N} \left([u_h (r_h)_t] - (\hat{r}_h)_t [u_h] - \hat{u}_h [(r_h)_t]\right)_{j+1/2} = 0.$$

(ii) From the conservation of energy E_2, we have

$$\|u_h\|^2 = E_2(t) - \|r_h\|^2 = E_2(0) - \|r_h\|^2 \le E_2(0).$$

Hence $\|u_h\|^2 \le E_2(0)$ as desired, and we have the L^2 stability. ∎

2.4. Time discretization. In this subsection, we develop fully discrete methods that maintain the invariant preserving property of the semidiscrete method (7). To achieve this, we will employ time stepping methods that preserve the discrete invariants. A family of symplectic temporal integrators which preserve the invariants up to round-off error is the implicit Runge–Kutta collocation type methods associated with the diagonal elements of the Padé table for e^z [12]. In this paper, we consider the second order midpoint rule and the fourth order two-stages Gauss–Legendre methods.

Let $\{t^n\}, n = 0, 1, \ldots, M$, be a uniform partition of the time interval $[0, T]$, and $\Delta t^n = t^{n+1} - t^n$. Let $u_h^0 = \Pi u_0$ be the piecewise L^2 projection of the initial condition $u_0(x)$. We update the solution u_h^{n+1} from u_h^n using the midpoint rule in the following manner: for $n = 0, \ldots, M-1$, $u_h^{n+1} \in V_h$ is given by

$$u_h^{n+1} = 2u_h^{n,1} - u_h^n, \tag{10}$$

where $u_h^{n,1}$ is the solution of the equation

$$u_h^{n,1} - u_h^n - \Delta t^n \mathcal{F}(u_h^{n,1}) = 0, \tag{11}$$

where $\mathcal{F}(u_h)$ is the spatial operator; see (13) for the fully discrete method. In Theorem 2.1, we have shown that the semidiscrete DG method preserves the continuous invariants $E_1(t)$ and $E_2(t)$. Along the same line of analysis, we can prove that the discrete invariants, as defined in the following theorem, is conserved by the fully discrete method.

Theorem 2.2. The fully discrete midpoint rule DG method (10)–(11) conserves the discrete invariants

$$E_1^n = \int m_h^n dx, \qquad E_2^n = \frac{1}{2}\int \left((u_h^n)^2 + (r_h^n)^2\right) dx \tag{12}$$

for all n.

Proof. Introduce the notation

$$\mathcal{D}m_h^n = \frac{m_h^{n+1} - m_h^n}{\Delta t^n} = \frac{m_h^{n,1} - m_h^n}{\Delta t^n/2}.$$

Combined with the DG formulation (9), the midpoint rule DG method (10)–(11) can be rewritten as

$$\int \mathcal{D}m_h^n \xi_h dx - \int q_h^{n,1}(\xi_h)_x dx - \sum_{j=1}^N \left(\widehat{q_h^{n,1}}[\xi_h]\right)_{j+1/2} + \int m_h^{n,1} r_h^{n,1} \xi_h dx = 0, \tag{13a}$$

$$\int (q_h^{n,1} - m_h^{n,1} u_h^{n,1})\eta_h dx = 0, \tag{13b}$$

$$\int m_h^{n,1}\rho_h dx - \int r_h^{n,1}(\rho_h)_x dx - \sum_{j=1}^N \left(\widehat{r_h^{n,1}}[\rho_h]\right)_{j+1/2} - \int u_h^{n,1}\rho_h dx = 0, \tag{13c}$$

$$\int r_h^{n,1}\psi_h dx + \int u_h^{n,1}(\psi_h)_x dx + \sum_{j=1}^N \left(\widehat{u_h^{n,1}}[\psi_h]\right)_{j+1/2} = 0. \tag{13d}$$

To show the conservation of E_1^n, we take the test functions $\xi_h = 1$ in (13a), $\rho_h = -r_h^{n,1}$ in (13c), and $\psi_h = -u_h^{n,1}$ in (13d), and sum the resulting relations to obtain

$$\begin{aligned}\int \mathcal{D}m_h^n dx = &- \int r_h^{n,1}(r_h^{n,1})_x dx - \sum_{j=1}^N \left(\widehat{r_h^{n,1}}[r_h]\right)_{j+1/2} + \int u_h^{n,1}(u_h^{n,1})_x dx \\ &+ \sum_{j=1}^N \left(\widehat{u_h^{n,1}}[u_h]\right)_{j+1/2} \\ = &\sum_{j=1}^N \left(\left(\{r_h^{n,1}\} - \widehat{r_h^{n,1}}\right)[r_h] - \left(\{u_h^{n,1}\} - \widehat{u_h^{n,1}}\right)[u_h]\right)_{j+1/2} = 0.\end{aligned}$$

Since $\int \mathcal{D}m_h^n dx = (E_1^{n+1} - E_1^n)/\Delta t^n$, we have $E_1^{n+1} = E_1^n$.

To show the conservation of E_2^n, we first consider (9c) at time levels t^n and t^{n+1}, and let the test function ρ_h be $-u_h^{n,1}/(\Delta t^n)$. Subtraction of these two equations yields

$$\int -\mathcal{D}m_h^n\, u_h^{n,1} dx + \int \mathcal{D}r_h^n\, (u_h^{n,1})_x dx + \sum_{j=1}^N \left(\widehat{\mathcal{D}r_h^n}[u_h^{n,1}]\right)_{j+1/2} + \int \mathcal{D}u_h^n\, u_h^{n,1} dx = 0. \tag{14}$$

We then take $\xi_h = u_h^{n,1}$ in (13a), $\eta_h = r_h^{n,1}$ in (13b), $\psi_h = \mathcal{D}r_h^n - q_h^{n,1}$ in (13d), and add the resulting equations with (14) to obtain

$$\int \left(\mathcal{D}u_h^n u_h^{n,1} + \mathcal{D}r_h^n r_h^{n,1}\right) dx = 0. \tag{15}$$

Combined with the fact that

$$\mathcal{D}u_h^n u_h^{n,1} = \frac{u_h^{n+1}-u_h^n}{\Delta t^n}\frac{u_h^{n+1}+u_h^n}{2} = \frac{\left(u_h^{n+1}\right)^2-(u_h^n)^2}{2\Delta t^n}, \qquad \mathcal{D}r_h^n r_h^{n,1} = \frac{\left(r_h^{n+1}\right)^2-(r_h^n)^2}{2\Delta t^n},$$

the relation (15) leads to $E_2^{n+1} = E_2^n$. ∎

In some of the numerical experiments with very high accuracy in spatial discretization, the following fourth order two-stages Gauss–Legendre methods, which also preserve the discrete invariants E_1^n and E_2^n, are conducted as the time approximations:

$$u_h^{n+1} = u_h^n + \sqrt{3}\left(u_h^{n,2} - u_h^{n,1}\right), \tag{16}$$

where $u_h^{n,1}$ and $u_h^{n,2}$ are given as solutions of the coupled system of equations

$$u_h^{n,1} - u_h^n - \Delta t^n\Big(a_{11}\mathcal{F}(u_h^{n,1}) + a_{12}\mathcal{F}(u_h^{n,2})\Big) = 0, \tag{17}$$

$$u_h^{n,2} - u_h^n - \Delta t^n\Big(a_{21}\mathcal{F}(u_h^{n,1}) + a_{22}\mathcal{F}(u_h^{n,2})\Big) = 0, \tag{18}$$

with $a_{11} = a_{22} = 1/4,\ a_{12} = 1/4 - \sqrt{3}/6,\ a_{21} = 1/4 + \sqrt{3}/6$.

2.5. Algorithm. In this section, we give details related to the implementation of the proposed invariant preserving DG method.

1. First, from (7d) and (7c), we obtain r_h and m_h in the following matrix form:

$$R_h = AU_h, \quad M_h = U_h - AR_h, \tag{19}$$

   where U_h (or R_h, M_h) denotes the vectors containing the degree of freedom for the piecewise polynomial solution u_h (or r_h, m_h). This leads to the following relation between M_h and U_h:

$$M_h = BU_h, \tag{20}$$

   with the matrix $B = I - A^2$.
2. Equation (7b) leads to q_h defined by

$$Q_h = \Pi(m_h u_h), \tag{21}$$

   where Π is the standard L^2 projection onto piecewise P^k polynomials.
3. Equation (7a) and (21) leads to

$$\partial_t M_h = -AQ_h - \Pi(m_h r_h). \tag{22}$$

4. We then combine (20) and (22) to obtain

$$\partial_t U_h = B^{-1}\left(-AQ_h - \Pi(m_h r_h)\right). \tag{23}$$

5. We apply a symplectic temporal discretization method, for example the second order midpoint method (10) or the fourth order Gaussian–Legendre method (16), to advance the obtained system (23) in time.

The differential matrix A is a sparse block matrix, hence its multiplication with coefficient vectors can be implemented efficiently. Step 5 involves a linear solver with the matrix B, where we can perform an LU decomposition for B at the beginning to save computational cost.

3. Numerical results. In this section we provide some numerical examples to illustrate the accuracy and capability of our method. The midpoint rule is used as the temporal discretization in most of the numerical results, except the accuracy test (Example 1) where the fourth order Gauss–Legendre methods are used. With the aid of successive mesh refinements we have verified that, in all cases, the results shown are numerically convergent.

Example 1 (accuracy test). The peaked traveling wave solution takes the form

$$u(x,t) = ce^{-|x-ct|}, \tag{24}$$

where $c = 0.25$ is the wave speed. The domain is set as $[-40, 40]$, and the accuracy is measured in the smooth parts of the solution, 1/20 of the computational domain away from the peak. We test the P^k polynomial approximation on uniform meshes. The L^2 errors and the numerical orders of accuracy for $k = 0, 1, 2$ at time $t = 1$ are reported in Table 1. The CFL condition is picked as 0.01. We can clearly see that the invariant preserving DG methods achieve the optimal convergence rates for P^k elements. The order of accuracy is a little oscillating around the optimal rate. This oscillating behavior of numerical accuracy is commonly observed for energy conserving methods, and a least square fitting of the order has been done in [26] and give the optimal convergence rate of u. In [6], carefully chosen numerical initial conditions are employed and optimal convergence rates are clearly observed there, which shows that the energy conserving method is more sensitive to the error in the initial conditions.

TABLE 1

Accuracy test of DG method for the CH equation with the exact solution (24). *The periodic boundary condition,* $c = 0.25$, *uniform meshes with* N *cells at time* $t = 1$.

	N	L^1 error	Order	N	L^2 error	Order	N	L^∞ error	Order
P^0	20	2.59e-03	-	20	1.09e-02	-	20	5.69e-02	-
	40	6.57e-04	1.98	40	4.88e-03	1.17	40	7.77e-02	-0.45
	80	2.48e-04	1.40	80	1.36e-03	1.84	80	2.06e-02	1.91
	160	1.19e-04	1.06	160	6.01e-04	1.18	160	8.20e-03	1.33
	320	5.74e-05	1.05	320	2.87e-04	1.07	320	3.86e-03	1.09
P^1	20	1.12e-03	-	20	5.45e-03	-	20	4.56e-02	-
	40	2.16e-04	2.37	40	2.06e-03	1.40	40	3.98e-02	0.20
	80	4.40e-05	2.30	80	2.55e-04	3.02	80	3.84e-03	3.37
	160	1.34e-05	1.72	160	6.74e-05	1.92	160	1.02e-03	1.90
P^2	20	6.46e-04	-	20	2.93e-03	-	20	3.17e-02	-
	40	1.31e-04	2.30	40	1.30e-03	1.18	40	2.86e-02	0.15
	80	8.71e-06	3.91	80	5.60e-05	4.53	80	8.81e-04	5.02
	160	1.42e-06	2.62	160	8.13e-06	2.79	160	1.15e-04	2.94

In the next four examples, the initial data will be generated from the following profiles:

$$\phi_i(x) = \begin{cases} \dfrac{c_i}{\cosh(a/2)} \cosh(x - x_i), & |x - x_i| \le a/2, \\ \dfrac{c_i}{\cosh(a/2)} \cosh(a - (x - x_i)), & |x - x_i| > a/2, \end{cases}$$

with c_i, x_i and a to be further specified.

Example 2 (peakon solution). In this example, we present the wave propagation of a single peak solution. The initial condition is given by

$$u_0(x) = \phi_0(x),$$

with the parameters $c_0 = 1$, $a = 30$, and $x_0 = -5$. We set the computational domain as $[0, a]$. The solution profile at time $t = 0$, 5, 10, and 20 are plotted in Figure 1. The lack of smoothness at the peak of peakons introduces high-frequency dispersive errors into the calculation, which will cause numerical oscillation near the peak. To resolve it, we use the P^4 polynomial with 200 cells.

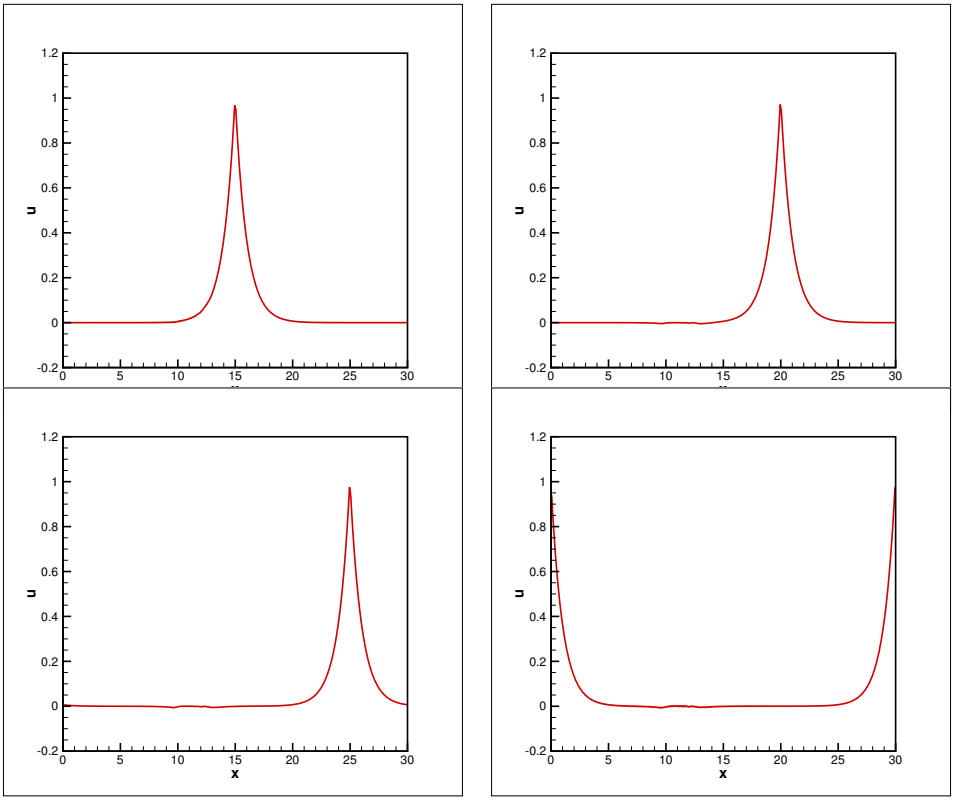

FIG. 1. *Example* 2, *peakon interaction: The solution at time* $T = 5$, 10, 15, *and* 20.

In Figure 2, we also provide the comparison of the conservative methods, compared with the energy dissipative LDG methods introduced by Xu and Shu [27] and the exact solutions. We can see a smaller phase error compared with the solutions from the energy dissipative methods.

The performance of conservative methods is expected to be better than dissipative methods for long time simulations, as observed for the DP equation in [21]. However, for the CH equation the improvement in terms of the phase error is not as good as that for the DP equation. This obvious phase error between the numerical solution and the exact solution is also observed in [22] when using the invariant preserving finite difference method.

Example 3 (two-peakon interaction). In this example, we consider the two-peakon interaction of the CH equation with the initial condition

$$u_0(x) = \phi_1 + \phi_2.$$

with $c_1 = 2$, $c_2 = 1$, $x_1 = -5$, $x_2 = 5$, and $a = 30$. We set the computational domain

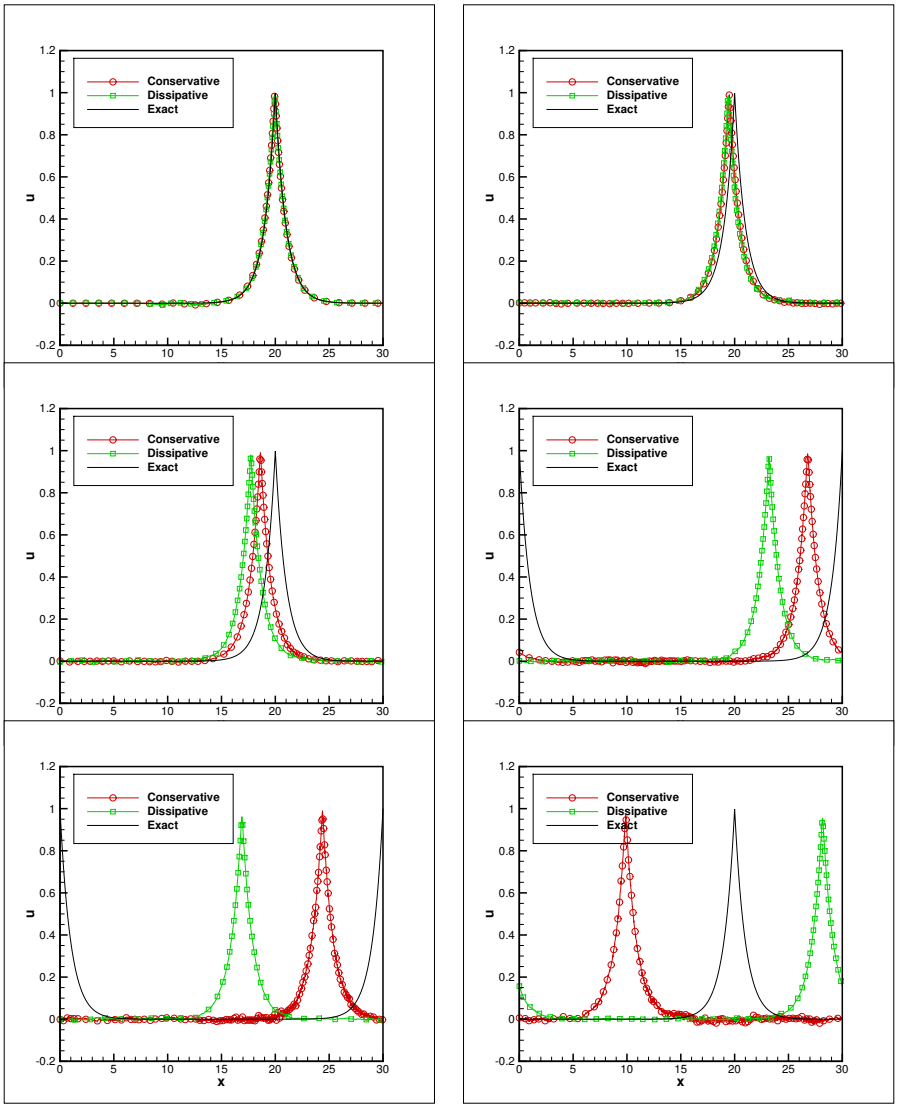

FIG. 2. *Example* 2, *Peakon interaction: The comparison of numerical solutions of energy conservative and energy dissipative DG methods at time* $T = 10$, 100, 250, 500, 740, *and* 1000.

as $[0, a]$. The solution profile at time $t = 5$, 10, 12, and 18 are plotted in Figure 3. We use the P^4 polynomial with 300 cells to resolve the peakon.

Example 4 (three-peakon interaction). In this example, we consider the three-peakon interaction of the CH equation with the initial condition

$$u_0(x) = \phi_1 + \phi_2 + \phi_3.$$

with $c_1 = 2$, $c_2 = 1$, $c_3 = 0.8$, $x_1 = -5$, $x_2 = -3$, $x_3 = -1$, and $a = 30$. We set the computational domain as $[0, a]$. The solution profile at time $t = 1$, 2, 3, 4, and 6 are plotted in Figure 4. Again, we use the P^4 polynomial with 300 cells to resolve the peakon.

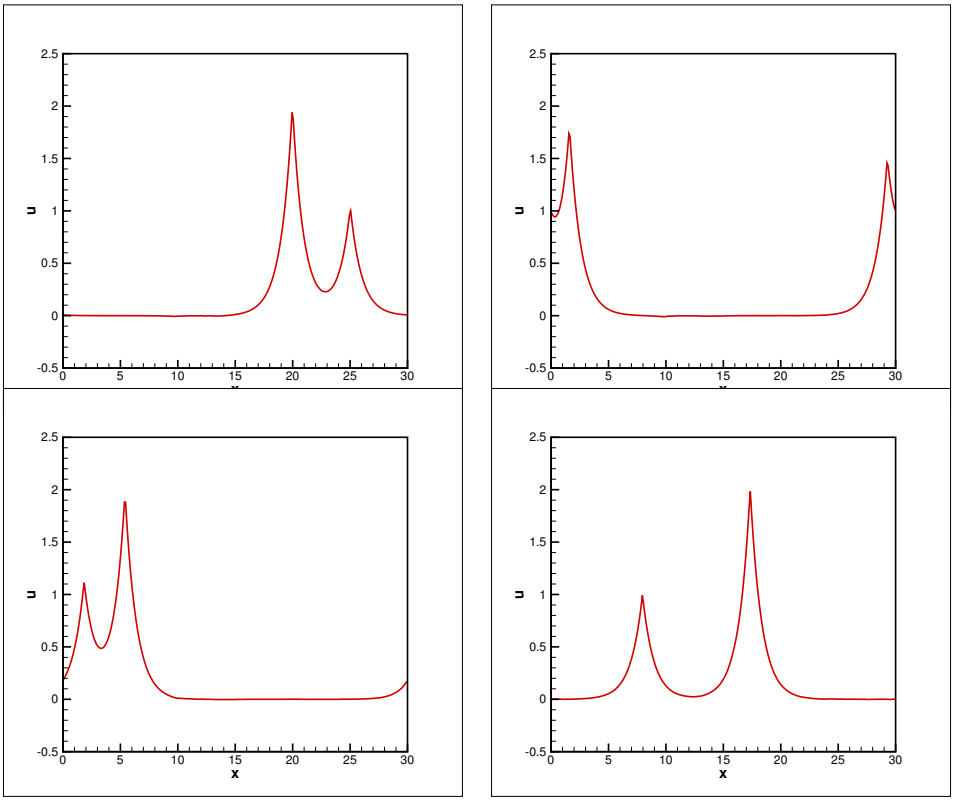

FIG. 3. *Example* 3, *two-peakon interaction: The solution at time* $T = 5$, 10, 12, *and* 18.

Example 5 (peakon-antipeakon interaction). In this example, we consider the interaction of peakon and antipeakon solutions of CH equation, with the initial condition given by

$$u_0(x) = \phi_1 + \phi_2.$$

with $c_1 = 1$, $c_2 = -1$, $x_1 = -7.5$, $x_2 = 7.5$, and $a = 30$. We set the computational domain as $[0, a]$. Since these two peakon solutions have the same magnitude but with opposite signs, the total momentum will remain zero, which is observed numerically during the simulations. The solution profile at time $t = 0$, 4, 6, 7, 8, and 10 are plotted in Figure 5. We use the P^4 polynomial with 300 cells to resolve the peakon.

Example 6 (nonpeakon solution). The initial data function contains a discontinuous derivative:

$$u_0(x) = \frac{10}{(3 + |x|^2)^2}.$$

We set the computational domain as $[-30, 30]$. The solution profile at time $t = 0$, 5, 10, and 20 are plotted in Figure 6. In this example, we use the P^2 polynomial with 600 cells for the simulation.

4. Conclusions. We have developed an invariant preserving DG scheme for the Camassa–Holm equation arising in the context of shallow water wave theory. The fully discrete scheme is shown to preserve both the momentum and total energy of the system. These ensure that the numerical solution provides a good long time

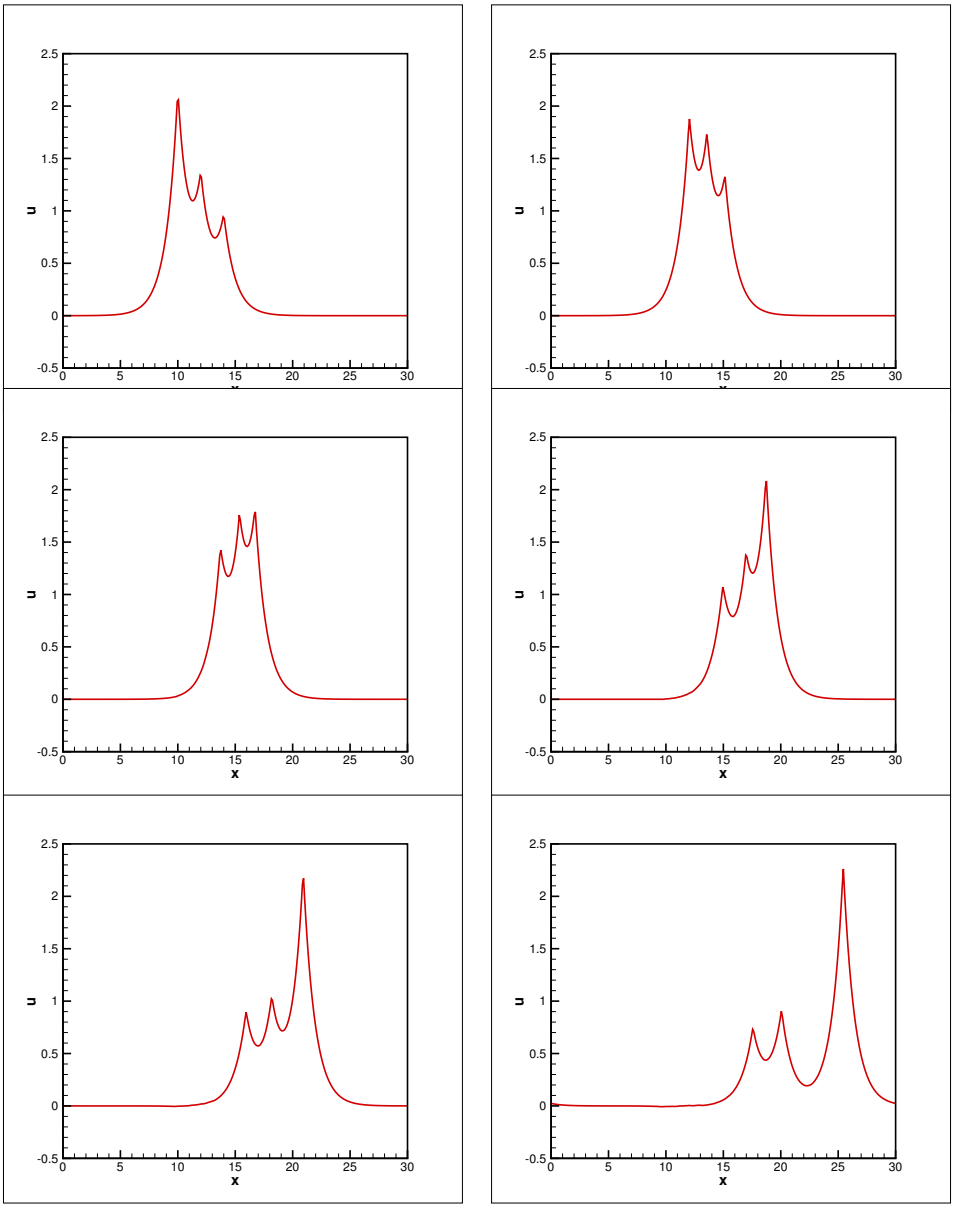

FIG. 4. *Example* 4, *three-peakon interaction: The solution at time* $T = 0$, 1, 2, 3, 4, *and* 6.

behavior, thus revealing the desired dispersal wave pattern of the underlying equation. Numerical examples are presented to illustrate both the accuracy and efficiency in simulating the CH equation. One future work is to investigate ways to further reduce

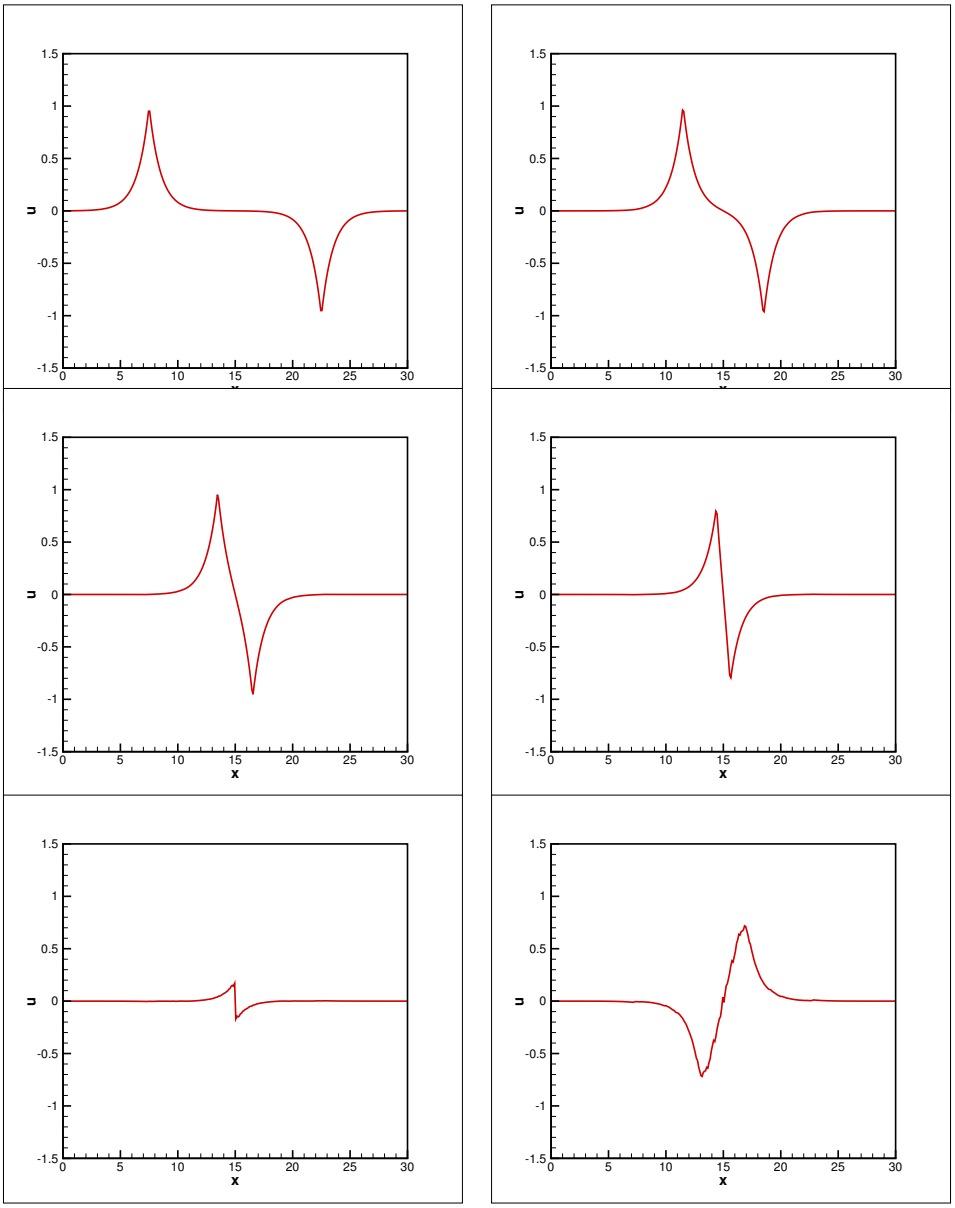

FIG. 5. *Example* 5, *peakon-antipeakon interaction: The solution at time* $T = 0$, 4, 6, 7, 8, *and* 10.

the phase error in long time simulations, and understand the different behaviors of invariant preserving DG methods for the CH and DP equations.

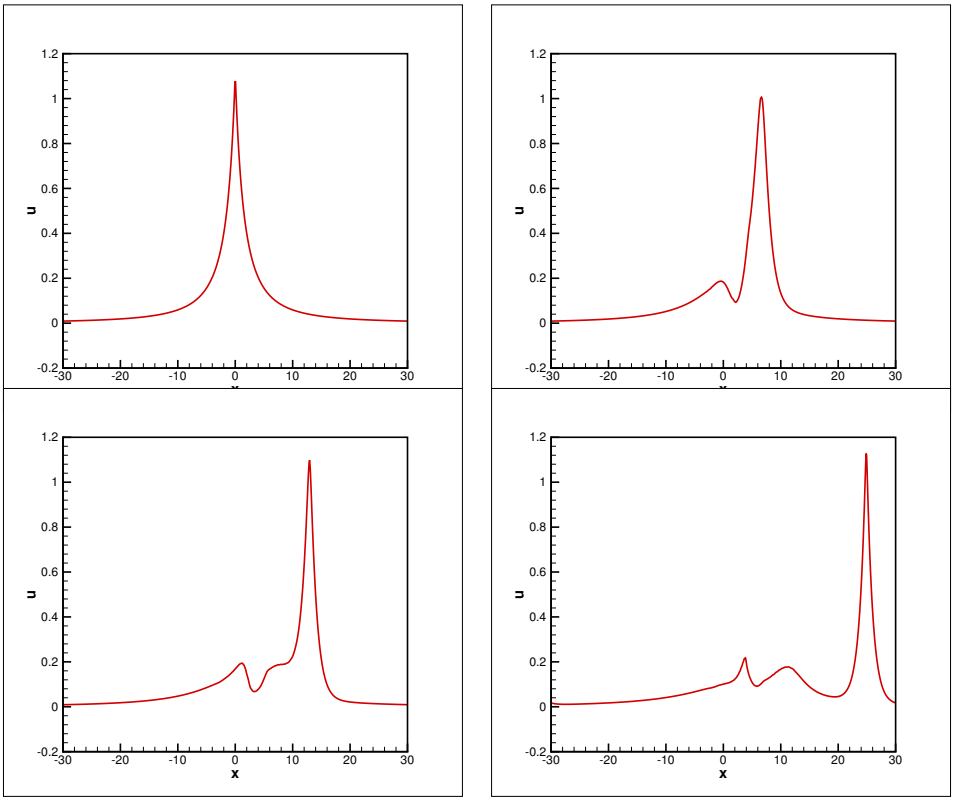

FIG. 6. *Example* 6*, solution with a discontinuous derivative: The solution at time* $T = 0$*,* 5*,* 10*, and* 20*.*

Acknowledgment. The second author is grateful to Yan Xu for providing the DG code in the paper [27].

REFERENCES

[1] D. APPELÖ AND T. HAGSTROM, *A new discontinuous Galerkin formulation for wave equations in second order form*, SIAM J. Numer. Anal. 53 (2015), pp. 2705–2726, doi: 10.1137/140973517.

[2] A. BRESSAN, G. CHEN AND Q.-T. ZHANG, *Uniqueness of conservative solutions to the Camassa–Holm equation via characteristics*, Discrete Contin. Dyn. Syst., 35 (2015), pp. 25–42.

[3] J. L. BONA, H. CHEN, O. KARAKASHIAN, AND Y. XING, *Conservative discontinuous Galerkin methods for the Generalized Korteweg–de Vries equation*, Math. Comp., 82 (2013), pp. 1401–1432.

[4] R. CAMASSA AND D. D. HOLM, *An integrable shallow water equation with peaked solitons*, Phys. Rev. Lett., 71 (1993), pp. 1661–1664.

[5] R. CAMASSA, D. D. HOLM, AND J. M. HYMAN, *A new integrable shallow water equation*, Adv. Appl. Mech., 31 (1994), pp. 1–33.

[6] C.-S. CHOU, C.-W. SHU, AND Y. XING, *Optimal energy conserving local discontinuous Galerkin methods for second-order wave equation in heterogeneous media*, J. Comput. Phys., 272 (2014), pp. 88–107.

[7] B. COCKBURN, G. KARNIADAKIS, AND C.-W. SHU, *The development of discontinuous Galerkin methods*, Discontinuous Galerkin Methods: Theory, Computation and Applications, Lect. Notes Comput. Sci. Eng. 11, Springer, Berlin, 2000, pp. 3–50.

[8] G. Coclite and K. Karlsen, *On the well-posedness of the Degasperis–Procesi equation*, J. Funct. Anal., 233 (2006), pp. 60–91.
[9] G. Coclite and K. Karlsen, *On the uniqueness of discontinuous solutions to the Degasperis–Procesi equation*, J. Differential Equations, 234 (2007), pp. 142–160.
[10] A. Constantin and D. Lannes, *The hydrodynamical relevance of the Camassa–Holm and Degasperis–Procesi equations*, Arch. Ration. Mech. Anal., 192 (2009), pp. 165–186.
[11] A. Degasperis, D. Holm, and A. Hone, *A new integrable equation with peakon solutions*, Theoret. and Math. Phys., 133 (2002), pp. 1463–1474.
[12] K. Dekker and J. G. Verwer, *Stability of Runge-Kutta Methods for stiff nonlinear differential equations*, North–Holland, Amsterdam, 1984.
[13] B. Fuchssteiner and A. S. Fokas, *Symplectic structures, their bäcklund transformations and hereditary symmetries*, Phys. D, 4 (1981), pp. 47–66.
[14] M. J. Grote, A. Schneebeli, and D. Schötzau, *Discontinuous Galerkin finite element method for the wave equation*, SIAM J. Numer. Anal., 44 (2006), pp. 2408–2431, doi: 10.1137/05063194X.
[15] T. G. Ha and H. Liu, *On traveling wave solutions of the θ-equation of dispersive type*, J. Math. Anal. Appl., 421 (2015), pp. 399–414.
[16] D. D. Holm and M. F. Staley, *Wave structure and nonlinear balances in a family of evolutionary PDEs*, SIAM J. Appl. Dyn. Syst., 2 (2003), pp. 323–380, doi:10.1137/S1111111102410943.
[17] R. S. Johnson, *Camassa–Holm, Korteweg–de Vries and related models for water waves*, J. Fluid Mech., 455 (2002), pp. 63–82.
[18] J. Lenells, *Traveling wave solutions of the Degasperis–Procesi equation*, J. Math. Anal. Appl., 306 (2005), pp. 72–82.
[19] H. Liu, *Wave breaking in a class of nonlocal dispersive wave equations*, J. Nonlinear Math. Phys., 13 (2006), pp. 441–466.
[20] H. Liu, *On discreteness of the Hopf equation*, Acta Math. Appl. Sin. Engl. Ser., 24 (2008), pp. 423–440.
[21] H. Liu, Y.-Q. Huang, and N.-Y. Yi, *A direct discontinuous Galerkin method for the Degasperis–Procesi equation*, Methods Appl. Anal., 21 (2014), pp. 83–106.
[22] H. Liu and T. Pendleton, *On invariant-preserving finite difference schemes for the Camassa–Holm equation*, Commun. Comput. Phys., 19 (2016), pp. 1015–1041.
[23] H. Liu and Z. Yin, *Global regularity, and wave breaking phenomena in a class of nonlocal dispersive equations*, Contemp. Math. 526, AMS, Providence, RI, 2011, pp. 273–294.
[24] H. Lundmark, *Formation and dynamics of shock waves in the Degasperis-Procesi equation*, J. Nonlinear Sci., 17 (2007), pp. 169–198.
[25] B. Riviere and M. F. Wheeler, *Discontinuous finite element methods for acoustic and elastic wave problems*, Contemp. Math. 329, AMS, Providence, RI, 2003, pp. 271–282.
[26] Y. Xing, C.-S. Chou, and C.-W. Shu, *Energy conserving local discontinuous Galerkin methods for wave propagation problems*, Inverse Probl. Imaging, 7 (2013), pp. 967–986.
[27] Y. Xu and C.-W. Shu, *A local discontinuous Galerkin method for the Camassa–Holm equation*, SIAM J. Numer. Anal., 46 (2008), pp. 1998–2021, doi:10.1137/070679764.
[28] Y. Xu and C.-W. Shu, *Local discontinuous Galerkin methods for high-order time-dependent partial differential equations*, Commun. Comput. Phys., 7 (2010), pp. 1–46.
[29] N.-Y. Yi, Y.-Q. Huang, and H. Liu, *A direct discontinuous Galerkin method for the generalized Korteweg–de Vries equation: Energy conservation and boundary effect*, J. Comput. Phys., 242 (2013), pp. 351–366.